

A thermodynamically consistent approach to modeling macroscopic solidification of binary systems

© S.A. Korobeynikov¹, D.M. Korobeynikov^{1,2}, V.G. Lebedev¹

¹ Udmurt Federal Research Center, Ural Branch Russian Academy of Sciences, Izhevsk, Russia

² Udmurt State University, Izhevsk, Russia

E-mail: sa.korobeynikov@yandex.ru

Received October 28, 2025

Revised December 23, 2025

Accepted January 20, 2026

A thermodynamically consistent macroscopic model of solidification of a binary system is hereby proposed. This model is based on the description of the evolution of the volume fraction as an advective quantity with a source. The system of equations is derived from the total entropy functional, thereby ensuring consistency between heat transfer, diffusion, and phase transformation. Numerical simulation for the Al–Mg system demonstrated congruence with the experimental DTA curve, thereby substantiating the model’s viability for macroscale depiction and prediction of solidification processes.

Keywords: solidification, binary systems, non-equilibrium thermodynamics, solidification kinetics.

DOI: 10.61011/TPL.2026.05.63288.20545

Numerical simulation of solidification processes on macroscopic scales relies predominantly on quasi-equilibrium approaches of the 1980s [1]. Prediction of phase composition and material properties remains heuristic to a great extent, and the use of computational thermodynamics potential [2] is limited. Hence it follows that the objective of the study is to develop and study a thermodynamically consistent macroscopic model of solidification of a binary two-phase system in the framework of dissipative thermodynamics, which is conceptually close to the phase field approach [3,4] and suitable for calculation of macroobjects.

We consider isothermal solidification of a binary two-phase system. For simplification, we assume that density doesn’t change during phase transition and the process runs at a constant pressure, which implies that there are no convective flows (and consequently shrinkage) and mechanical stresses.

We introduce a concept of the order parameter $\varphi(\mathbf{r}, t)$ expressed as a volume fraction of a phase that occupies a point in space. Volume fraction interval is limited to $\varphi \in [0; 1]$, and the intermediate values correspond to a physical two-phase mixture, unlike classical phase field approaches [3]. $\varphi = 1$ and $\varphi = 0$ are hereinafter referred to as full filling with a solid phase (S) and a liquid phase (L), respectively.

To clarify a physical and mathematical basis, we consider an idealized system with pre-defined thermal and solutal undercooling. Solid volume fraction grows at a constant rate proportional to the thermodynamic motive force; the φ profile uniformly moves, absorbing a higher-energy phase (parallel transfer). Adjacent cells are directly interconnected: crystallite (dendrites) grow into them and implement the transfer.

Advection equation with a source can serve as an obvious mathematical formulation of such idealized process

$$\dot{\varphi} = -\mathbf{V} \cdot \nabla \varphi + Q, \quad (1)$$

where \mathbf{V} is the rate of volume filling with the solid phase, rather than a classical rate associated with the convective transfer. The proposed equation already considers two growth mechanisms: crystallite growth into adjacent cells (profile transfer) and local growth/dissolution driven by the source Q .

To derive equations of non-isothermal solidification process relaxation, we write the total system entropy functional

$$S = - \int_V \frac{\partial g}{\partial T} dV, \quad g = \varphi g^S(x_S, T) + (1 - \varphi) g^L(x_L, T),$$

where g^S and g^L are bulk densities of Gibbs energy of the solid phase (S) and liquid phase (L), respectively. Function arguments are hereinafter omitted for brevity.

To account for heat transfer, we use the heat conservation law (enthalpy) where the density of enthalpy h is expressed through the Gibbs energy density.

$$\frac{\partial h}{\partial t} = -\nabla \cdot \mathbf{J}_T, \quad h = g - T \frac{\partial g}{\partial T}. \quad (2)$$

Expanding expression (2) and substituting corresponding summands into the derivative of S with respect to time, we get

$$\frac{dS}{dt} = - \int_V \left[\frac{1}{T} \Delta g \dot{\varphi} + \frac{1}{T} \nabla \cdot \mathbf{J}_T + \frac{1}{T} \mu^S \varphi \dot{x}_S + \frac{1}{T} \mu^L (1 - \varphi) \dot{x}_L \right] dV,$$

where $\Delta g = g^S - g^L$, and μ^S and μ^L are chemical potentials defined as partial derivatives of Gibbs energy densities with respect to corresponding molar fractions.

A component conservation law is formulated in the same way. As the impurity is redistributed between phases during the phase transition, a mean molar fraction $\langle x \rangle = \varphi x_S + (1 - \varphi)x_L$ is retained, rather than separate x_S, x_L . Separating by phases [4,5], we have

$$\varphi \dot{x}_S = -\Delta x \dot{\varphi} \Theta(\dot{\varphi}) - \nabla \cdot \mathbf{J}_S - R,$$

$$(1 - \varphi) \dot{x}_L = -\Delta x \dot{\varphi} \Theta(-\dot{\varphi}) - \nabla \cdot \mathbf{J}_L + R,$$

where $\Delta x = x_S - x_L$, $\Theta(\dot{\varphi})$ is the Heaviside function. Such partition implies that the total diffusion flux is a sum of fluxes in each of the phases: $\mathbf{J}_D = \mathbf{J}_S + \mathbf{J}_L$; „kinetic“ contribution of $\propto \dot{\varphi}$ is present in both equations and is localized by the Heaviside function in the growing phase (impurity trapping by the „oncoming phase“); a dissipative source R responsible for interphase impurity exchange is introduced. Their sum gives the initial conservation law

$$\frac{\partial}{\partial t} \langle x \rangle = -\nabla \cdot \mathbf{J}_D.$$

Substituting the derived equations into (3), applying Gauss's theorem to divergence terms, omitting the surface integral, replacing $\dot{\varphi}$ from kinetic equation (1), we get an expression for the rate of change of the total entropy

$$\begin{aligned} \frac{dS}{dt} = \int_V & \left[\mathbf{V} \frac{1}{T} \Delta \Omega \nabla \varphi - Q \frac{1}{T} \Delta \Omega - \mathbf{J}_S \nabla \left(\frac{\mu^S}{T} \right) \right. \\ & \left. - \mathbf{J}_L \nabla \left(\frac{\mu^L}{T} \right) + R \frac{\mu^S - \mu^L}{T} + \mathbf{J}_T \nabla \left(\frac{1}{T} \right) \right] dV, \end{aligned}$$

where $\Delta \Omega = g^S - g^L - \mu^{eff}(x_S - x_L)$ is the thermodynamic source depending on the phase transition direction, and μ^{eff} is the effective chemical potential (see [5,6]).

Following the non-equilibrium thermodynamics principles [7] and requiring an increase in the entropy bulk contribution, we get linear Onsager relations for fluxes

$$\begin{aligned} \mathbf{V} &= M_V \frac{1}{T} \Delta \Omega \nabla \varphi, & Q &= -M_Q \frac{1}{T} \Delta \Omega, \\ \mathbf{J}_{S,L} &= -M_D^{S,L} \nabla \left(\frac{\mu^{S,L}}{T} \right), & R &= M_R \frac{\mu^S - \mu^L}{T}, \\ \mathbf{J}_T &= -M_T \frac{1}{T^2} \nabla T, \end{aligned}$$

where $M_V > 0$, $M_Q > 0$, $M_D^{\{S,L\}} > 0$, $M_R > 0$, $M_T > 0$ are mobilities. The obtained expressions have direct physical interpretation. Contributions of \mathbf{V} and Q to the change of volume fraction are proportional to deviation from the phase equilibrium $\Delta \Omega$. Dissipative source R is defined by the difference of chemical potentials and, consequently, is also proportional to deviation from the diffusion equilibrium.

Using the freedom in choosing mobilities and maintaining dissipativity, we replace

$$M_V \rightarrow \frac{M_V T_c}{|\nabla \varphi|}, \quad M_Q \rightarrow M_Q T_c \varphi (1 - \varphi), \quad M_T \frac{1}{T^2} \rightarrow \kappa,$$

$$M_D^S \rightarrow M_D^S \varphi, \quad M_D^L \rightarrow M_D^L (1 - \varphi), \quad M_R \rightarrow M_R T_c \varphi (1 - \varphi),$$

where T_c is the normalizing temperature, $|\nabla \varphi|$ is the absolute value of the volume fraction profile gradient, κ is the thermal conductivity coefficient (replacement reduces \mathbf{J}_T to Fourier's law); φ and $(1 - \varphi)$ localize the contribution by phases and zero the sources beyond their determination region.

Introduction of $|\nabla \varphi|$ makes it possible to represent the „filling rate“ as a product of a normal component and unit normal vector

$$\mathbf{V} = M_V \frac{T_c}{T} \Delta \Omega \mathbf{n} = V_n \mathbf{n}.$$

Expanding the divergence in the expressions for diffusion fluxes and neglecting $\propto \nabla T$ for simplicity, we relate $M_D^{\{S,L\}}$ with the corresponding diffusion constants $D^{\{S,L\}}$, obtaining „classical“ Fick's law for different phases

$$D^{\{S,L\}} = \frac{M_D^{\{S,L\}}}{T} \frac{\partial \mu^{\{S,L\}}}{\partial x_{\{S,L\}}},$$

$$\mathbf{J}_S = -\varphi D^S \nabla x_S, \quad \mathbf{J}_L = -(1 - \varphi) D^L \nabla x_L.$$

In the final version, an equation of thermal conductivity with sources (difference of enthalpy densities — latent heat release during crystallization and thermal effect from a change of impurity concentration due to diffusion and exchange between phases) is added to the equation of volume fraction evolution and pair equations for molar fractions in phases

$$C_p \dot{T} = \nabla \cdot (\kappa \nabla T) - \dot{\varphi} (h^S - h^L) - \dot{x}_S \varphi \frac{\partial h^S}{\partial x_S} - \dot{x}_L (1 - \varphi) \frac{\partial h^L}{\partial x_L}.$$

For basic model verification, numerical simulation was performed with evaluation of the thermal effect of phase transition and comparison with the experimental differential thermal analysis (DTA) curve. As one-dimensional problem in the region $x \in [x_1, x_2]$ was considered as trial statement: temperature at one end decreased at a constant rate, the opposite end of the interval is heat insulated, temperature at the „cold“ boundary was taken as the reference.

To improve calculation feasibility, experimental molar Gibbs energies of the Al–Mg system were used [8], and the molar volume required for dimension matching was calculated using the data from [9]. An aluminum-enriched region ($x_{\{S,L\}}$ — molar fractions of Mg), where the FCC phase and liquid phase interact, was considered. Experimental functions for $D^{\{S,L\}}$ from [10] were used. Other simulation parameters are listed in the table. M_V , M_Q and M_R were selected manually using the data from a particular experiment.

Numerical simulation parameters

Parameter	Designation	Value
Thermal conductivity, W/(m · K)	κ	120
Level transfer mobility, m ⁴ /(J · s)	M_V	$3 \cdot 10^{-11}$
Bulk growth mobility, m ³ /(J · s)	M_Q	10^{-12}
Impurity redistribution mobility, m ³ /(J · s)	M_R	10^{-11}
Spatial interval, m	$x_1 - x_2$	$0 - 10^{-2}$
Dimensional parameter of space, m	L	10^{-3}
Normalization temperature, K	T_c	900
Dimensionless space step	$\Delta\xi$	0.01
Dimensionless time step	$\Delta\tau$	10^{-6}

For numeric solution, the system of equations was reduced to a dimensionless form and solved by the method of finite differences. Volume fraction equation was integrated by a semi-implicit sweep method using Godunov's scheme; diffusion equation was integrated in an implicit conservative form with regularization ($\varepsilon_{reg} = 10^{-6}$) to prevent division by zero; thermal conductivity equation was integrated by a semi-implicit sweep method. The Heaviside function was approximated by a smoothed hyperbolic tangent: $\Theta(\phi) = 0.5(1 + \tanh(\phi/\varepsilon_\Theta))$, smearing parameter $\varepsilon_\Theta = 10^{-6} \cdot \max(|\dot{\phi}|)$.

Initial and boundary conditions were set as follows:

$$\begin{aligned} \varphi(x, 0) &= 10^{-3}, & \varphi(x_1, t) &= 1, & \varphi'(x_2, t) &= 0, \\ x_{\{S,L\}}(x, 0) &= 0.0748, & x'_{\{S,L\}}(x_1, t) &= x'_{\{S,L\}}(x_2, t) = 0, \\ T(x, 0) &= 905 \text{ K}, & T(x_1, t) &= 905 \text{ K} - 20 \text{ K/min} \cdot t, \\ & & T'(x_2, t) &= 0. \end{aligned}$$

Figure 1 shows distributions at the heat release peak time. Profile φ moves to the opposite boundary of the region, which corresponds to directional growth of the solid phase and to release of supercooling. Molar fractions in phase tend to equilibrium values corresponding to the liquidus and solidus lines. Temperature profile shows heat accumulation in the right-hand part of the region due to crystallite intergrowth.

Figure 2 shows the experimental DTA curve from [11] (input data were provided by the authors) and the calculated dependence of ΔT between the sample boundaries on the „cold“ end temperature. Simulation shows both qualitative and quantitative agreements with experiment; despite the difference in conditions, the curves are in agreement.

This work proposes a thermodynamically consistent macroscopic model of binary system solidification based on description of the behavior of the phase volume fraction φ as an advective quantity with a source. Derivation of a system of equations from the total entropy functional ensured internal consistency of the model and linked the impurity redistribution and heat transfer processes to the phase composition evolution. The given statement implies the description of diffusion solidification in the stationary melt (without convection), which limits the scope of

the model to problems without substantial hydrodynamic effects. Consideration of natural convection and related processes will require introduction of additional convective contributions and modification of the φ field evolution equation, which is seen as the future research area.

The numerical simulation has proved the physical reliability of the approach and demonstrated good coincidence with the experimental DTA curve both in shape and typical

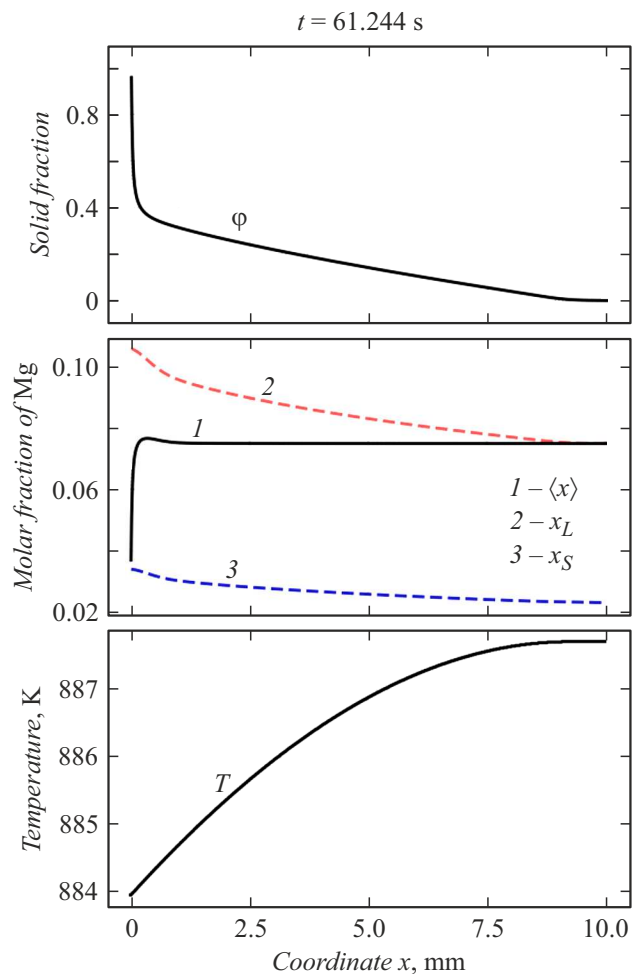


Figure 1. $\varphi(x, t)$, $\langle x \rangle$, $x_{\{S,L\}}(x, t)$, $T(x, t)$ field profiles of the Al–Mg system at time corresponding to the region of maximum ΔT .

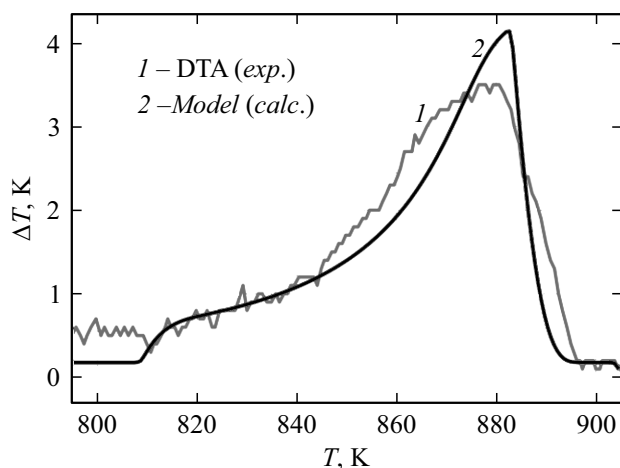


Figure 2. Experimental and computational profiles of thermogram $\Delta T(T)$ for $\text{Al}_{92.5}\text{Mg}_{7.5}$ alloy at a cooling rate of 20 K/min.

scales. Further adjustment of numerical experiment and optimization of M_V , M_Q and M_R taking into account their temperature and concentration dependence on the basis of advanced experiment will make it possible to improve the accuracy of prediction and extend the model to problems with complex geometry and thermal kinetics, thus forming the basis for a new class of macroscopic solidification models in the non-equilibrium thermodynamics framework.

Funding

The study was supported by grant No 25-22-20002 awarded by the Russian Science Foundation (<https://rscf.ru/project/25-22-20002>).

Conflict of interest

The authors declare no conflict of interest.

References

- [1] V.A. Zhuravlev, *Zatverdevanie i kristallizatsiya splavov s geteroperekhodami* (Regulyarnaya i khaoticheskaya dinamika, Izhevsk–M., 2006) (in Russian).
- [2] M. Hillert, *Phase equilibria, phase diagrams and phase transformations* (Cambridge University Press, Cambridge, 2008).
- [3] W.J. Boettinger, J.A. Warren, C. Beckermann, A. Karma, *Annu. Rev. Mater. Res.*, **32** (1), 163 (2002). DOI: 10.1146/annurev.matsci.32.101901.155803
- [4] S.G. Kim, W.T. Kim, T. Suzuki, *Phys. Rev. E*, **60** (6), 7186 (1999). DOI: 10.1103/PhysRevE.60.7186
- [5] V.G. Lebedev, *JETP Lett.*, **115** (4), 226 (2022). DOI: 10.1134/S0021364022040075.
- [6] M. Hillert, M. Rettenmayr, *Acta Mater.*, **51** (10), 2803 (2003). DOI: 10.1016/S1359-6454(03)00085-5
- [7] S.R. de Groot, P. Mazur, *Non-equilibrium thermodynamics* (Dover Publ., N.Y., 1984).

- [8] Y. Zuo, Y.A. Chang, *Calphad*, **17** (2), 161 (1993). DOI: 10.1016/0364-5916(93)90017-6
- [9] D. Huang, S. Liu, Y. Du, *Calphad*, **68**, 101693 (2020). DOI: 10.1016/j.calphad.2019.101693
- [10] Y. Du, Y. Chang, B. Huang, W. Gong, Z. Jin, H. Xu, Z. Yuan, Y. Liu, Y. He, F.-Y. Xie, *Mater. Sci. Eng. A*, **363** (1/2), 140 (2003). DOI: 10.1016/s0921-5093(03)00624-5
- [11] E.A. Batalova, L.V. Kamaeva, *Khimicheskaya fizika i mezoskopiya*, **23** (3), 29 (2021)(in Russian). DOI: 10.15350/17270529.2021.3.29

Translated by E.Ilyinskaya